

Formation mechanisms of quantum dots in the Sn/Si system

Peter Möck*, Yuanyuan Lei, Teya Topuria, and Nigel D. Browning

Department of Physics, University of Illinois at Chicago, 845 W. Taylor Street, Chicago, Illinois 60607-7059, * now at: Portland State University, Department of Physics, P.O. Box 751, Portland, OR 97207-0751; tel.: 312 497 4424, e-mail: peter_moeck@hotmail.com, pmoeck@uic.edu

Regina Ragan, Kyu S. Min***, and Harry A. Atwater**

Thomas J. Watson Laboratory of Applied Physics, California Institute of Technology, MS 128-95, Pasadena, CA 91125, ** now at Hewlett-Packard Laboratories M/S 1123, 1501 Page Mill Rd, Palo Alto, CA 94304, *** now at Intel Corporation, California Technology and Manufacturing, MS RNB-2-35, 2200 Mission College Blvd, Santa Clara, CA 95052-8119

Transmission electron microscopy in both the parallel illumination and scanning probe mode revealed the existence of two mechanisms for the formation of quantum dots in the Sn/Si system. Both mechanisms are believed to operate simultaneously during temperature and growth rate modulated molecular beam epitaxy combined with ex situ thermal treatments. One of the mechanisms involves the creation of voids in Si, which are subsequently filled by endotaxially grown Sn, resulting in QD that consist of pure α -Sn. The other mechanism involves phase separation and probably leads to substitutional solid solutions with a much higher Sn content than the predecessor quantum well structure possesses. In both cases, the quantum dots possess the diamond structure, the typical shape of a tetrakaidecahedron, and an excess Gibbs free energy of approximately 1.5 eV per atom due to compressive lattice mismatch strains.

1. Introduction

Self-assembled semiconductor quantum dots (QDs) are expected to lead to “*paradigm changes in semiconductor physics*” [1]. For semiconductor opto-electronic devices, the QDs must be sized on the order of the exciton Bohr radius for quantum confinement of carriers with an energy bandgap smaller than the surrounding semiconductor matrix. No structural defects (such as dislocations) which lead to non-radiative recombinations of the bound states of electrons and holes are allowed to exist in the QDs [2].

As α -Sn is a direct, ~ 0.08 eV, band gap semiconductor and substitutional solution $\text{Sn}_x\text{Si}_{1-x}$ are predicted to possess direct band gaps for $0.9 < x < 1$ [3], QDs in a Si matrix consisting of pure α -Sn or $\text{Sn}_x\text{Si}_{1-x}$ with a sufficiently high Sn content have potential applications as direct band-gap material for cheap and effective optoelectronics and thermo-photovoltaic devices. There are, however, a 19.5 % lattice mismatch between α -Sn and Si and an equilibrium solid solubility of Sn in Si of only 0.12 % at room temperature, that restrict growth of pseudomorph $\text{Sn}_x\text{Si}_{1-x}$ layers on Si by molecular beam epitaxy (MBE) [4-7] to a Sn content of about 10 % and a thickness of the order of magnitude of 10 nm.

At growth temperatures in the range 220 to 295 °C, pseudomorph $\text{Sn}_x\text{Si}_{1-x}$ layers with up to 5 % Sn content have been grown with film thicknesses up to 170 nm. Thermal treatments of these layers at temperatures above 500 °C for 1 hour lead to the formation of α -Sn precipitates, β -Sn precipitates, precipitates that consisted of both α -Sn and β -Sn, and misfit dislocations [5-7]. While these α -Sn precipitates may be considered to constitute QDs in this system (according to the requirements given above), the simultaneously present misfit dislocations are clearly undesirable for device applications.

Alternatively, temperature and growth rate modulated MBE [8,9] produces $\text{Sn}_x\text{Si}_{1-x}/\text{Si}$ superlattices with essentially pseudomorph $\text{Sn}_x\text{Si}_{1-x}$ substitutional solutions having Sn composition in the range of $x = 0.02$ to 0.05 and film thickness ranging from 1 to 2 nm. The growth temperatures of the $\text{Sn}_x\text{Si}_{1-x}$ layers ranged from 140 to 170 °C and the growth rate was 0.02 nm per second. To prevent segregation of Sn to the surface during growth, the $\text{Sn}_x\text{Si}_{1-x}$ layers were overgrown with 4 to 6 nm of Si at the $\text{Sn}_x\text{Si}_{1-x}$ growth temperature and at growth rates ranging from 0.01 to 0.03 nm per second. The temperature was then raised to 550 °C and a Si capping layer with a thickness of the order of magnitude 100 nm was grown at a rate of 0.05 nm per second. By the time this growth sequence has

been completed, the $\text{Sn}_x\text{Si}_{1-x}$ layer has experienced an *in situ* thermal treatment at 550 °C for a time of the order of magnitude 30 minutes. For the growth of $\text{Sn}_x\text{Si}_{1-x}/\text{Si}$ multilayer structures, the whole growth sequence was repeated several times, effectively resulting in an *in situ* thermal treatment for the first $\text{Sn}_x\text{Si}_{1-x}$ layer at 550 °C for a time on the order of magnitude a few hours [8,9]. In addition to this *in situ* thermal treatment, *ex situ* anneals at temperatures between 550 and 900 °C were performed for 30 minutes.

There are some uncertainties as to the formation mechanisms and crystallographic phases of the QDs that result from temperature and growth rate modulated MBE. Employing transmission electron microscopy in both the parallel and scanning probe mode, we will address these two issues in the main part of this paper. Thermodynamically driven structural transformations may occur over time in such QDs as one can easily estimate [10] that there is an essentially hydrostatic pressure in the GPa range [11] on these entities with a corresponding excess Gibbs free energy of approximately 1.5 eV per atom. This excess Gibbs free energy may be reduced or eliminated by structural transformations from α -Sn to β -Sn or from $\text{Sn}_x\text{Si}_{1-x}$ alloys into ordered Sn-Si compounds over a long enough time, even at room temperature. Here we would like to mention only that we actually observed in the above mentioned samples β -Sn precipitates and other yet unidentified precipitates that may have come into being by means of such structural transformations [12].

2. Experimental details

Three sets of pairs of multilayer samples (one with and one without an additional ex-situ anneal for 30 minutes at 800 °C) with four $\text{Sn}_x\text{Si}_{1-x}/\text{Si}$ layers and substitutional Sn contents of nominally 2 %, 5 %, and 10 % in each of the $\text{Sn}_x\text{Si}_{1-x}$ layers were grown by temperature and growth rate modulated MBE [8,9], stored at room temperature for a few years, and eventually selected for our TEM investigations.

Our structural analyses employed TEM in both the parallel illumination and scanning probe mode using a JEOL JEM-2010F Schottky field emission STEM/TEM and a JEOL JEM-3010 TEM. Parallel illumination TEM utilized conventional diffraction contrast (CTEM) and high-resolution phase contrast (HRTEM) imaging. Atomic resolution Z-contrast imaging in the scanning probe mode (STEM) proved to be especially useful for our investigations as the effects of strain fields in and around QDs and interference effects such as the formation of moiré fringe due to double diffraction are negligible. TEM specimen preparation followed standard procedures involving mechanical grinding and ion milling to electron transparency.

3. Results and Discussions

Fig. 1a shows a $\text{Sn}_{0.1}\text{Si}_{0.9}$ multilayer structure in a CTEM overview and Fig. 1b shows the structure in a Z-contrast STEM overview. While the $\text{Sn}_{0.1}\text{Si}_{0.9}$ layers appear dark in the CTEM images (due to strain field influences and a combination of diffraction and absorption contrast), the Z-contrast image shows these layers brighter than the surrounding Si matrix since the average atomic number in these layers is much larger than that of Si. Most of the Sn QDs formed at or in close proximity to the $\text{Sn}_{0.1}\text{Si}_{0.9}$ layers, but there are also many Sn QDs that grew within the Si spacer layers.

Figs. 2a and b show HRTEM images of structurally defective and perfectly pseudomorph $\text{Sn}_x\text{Si}_{1-x}$ layers in Si, respectively. The defect density was observed to decrease with the nominal Sn content in the $\text{Sn}_x\text{Si}_{1-x}$ layers. Samples with a nominal Sn content equal to or less than 5 % in the $\text{Sn}_x\text{Si}_{1-x}$ layers were found to be essentially free of defects.

Earlier plan-view TEM investigations of essentially defect free $\text{Sn}_x\text{Si}_{1-x}$ layers annealed at 650 °C revealed an initially rapid increase of the average Sn QD volume ($\langle r \rangle^3$) with time (t) for the first 2.2 hours of the anneal, Fig. 3 [9]. After this time, the function $\langle r \rangle^3(t)$ showed the typical linear behavior that is expected for precipitate coarsening by volume diffusion [13]. Textbook knowledge [13] attributes non-linearities of $\langle r \rangle^3$ with t to diffusion shortcuts such as dislocations, stacking faults, grain boundaries, and other common lattice defects.

Z-contrast STEM imaging in atomic resolution, Figs. 4a,b and 5a, however, revealed that within the Si matrix quite far away from the spatial positions of the $\text{Sn}_x\text{Si}_{1-x}$ layers (see also Figs. 1a,b), there are many voids in the Si matrix which are partly filled by Sn in both *ex situ* annealed and as grown samples (that had only had *in situ* thermal treatments). Fig. 5a is especially instructive as one can see that Sn lines the interface between the void and the Si matrix. Additional evidence for the existence of voids in Si that are partly filled with Sn has been gathered by quantitative electron energy loss spectroscopy and will be presented elsewhere [14]. We consider such voids as preferential sinks for diffusing Sn atoms, i.e. as very likely candidates for the above mentioned diffusion shortcuts.

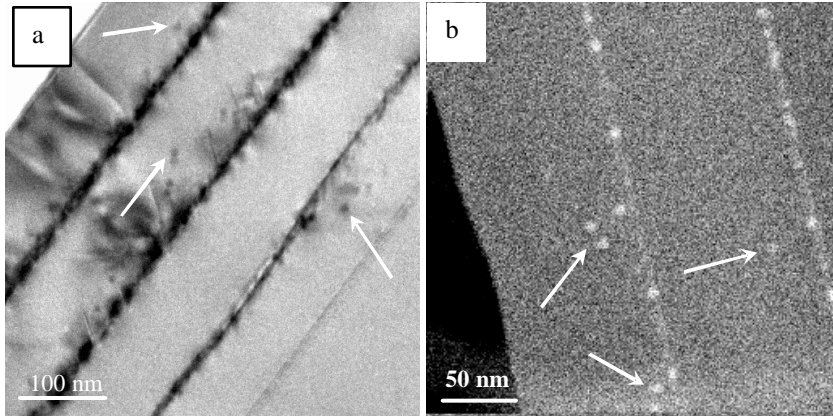


Figure 1: $\text{Sn}_{0.1}\text{Si}_{0.9}/\text{Si}$ multilayer structures in [110] cross sections, additional *ex situ* anneal; the arrows points towards QDs that grew within the Si layer; **(a)** CTEM overview; **(b)** Z-contrast STEM overview.

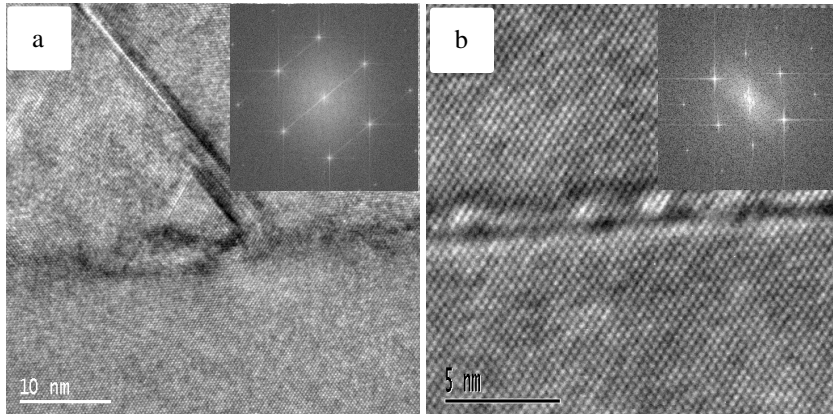


Figure 2: [110] cross section HRTEM images with power spectra inserts; **(a)** $\text{Sn}_{0.1}\text{Si}_{0.9}$ layer (arrow) with lattice defects on $\{111\}$ and $\{1\bar{1}1\}$ planes, as deposited (i.e. only *in situ* thermal treatments); **(b)** $\text{Sn}_{0.02}\text{Si}_{0.98}$ layer as deposited.

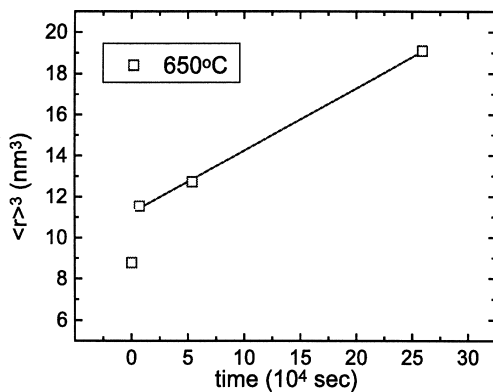


Figure 3: Results of earlier *ex situ* annealing experiments at 650 °C, after ref. [9]. The plot of the average QD size ($\langle r \rangle^3$) over the annealing time (t) shows that within the first 2.2 hours, the volume of the QDs increases very rapidly. Later on, the $\langle r \rangle^3(t)$ function shows the typical linear relationship that is expected when the precipitate coarsening is governed by volume diffusion. We attribute the initial rapid increase of the average QD size to diffusion shortcuts such as voids in the Si matrix.

It is now important to realize that the equilibrium shape of a void in Si has been determined experimentally [15] to be a tetrakaidecahedron, Fig. 6. The applications of Neumann's symmetry principle [16,17] to the determination of the shape of a-Sn precipitates in a Si matrix shows that this can be a tetrakaidecahedron as well.

Filling a void in Si with Sn by means of diffusion (into a diffusion shortcut) as a result of an additional thermal treatment at moderate parameters (300 °C for approximately three hours) directly in the electron microscope resulted in an a-Sn QD, Fig. 4b, as a-Sn and Si both possess the diamond structure. We consider this observation as direct proof of the void-filling hypothesis presented above.

This mechanism also provides a straightforward explanation for the initially rapid increase of the average Sn QD volume with annealing time in Fig. 3. The creation of voids in Si and subsequent filling with Sn emerges, therefore, as the first of the two mechanisms by which quantum dots in the Sn/Si system form.

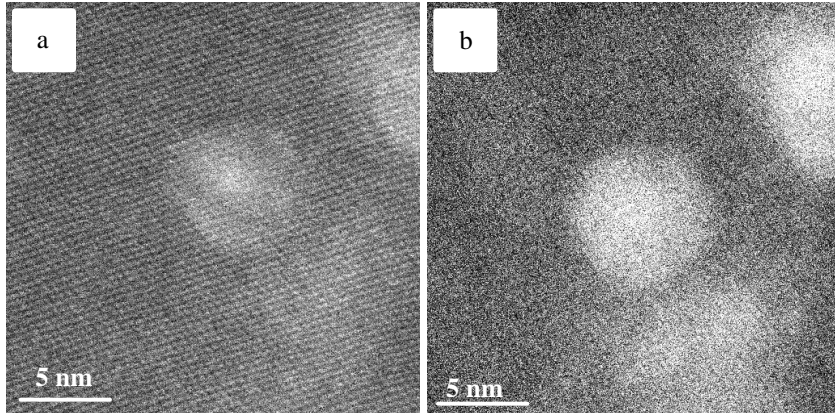


Figure 4: [110] cross section Z-contrast STEM images of a voids in Si, $x = 0.05$, ex-situ anneal; (a) partially filled with a-Sn; (b) filled with more a-Sn and grown in size as a result of a moderate additional thermal treatment inside the microscope (300 °C for approximately 3 hours).

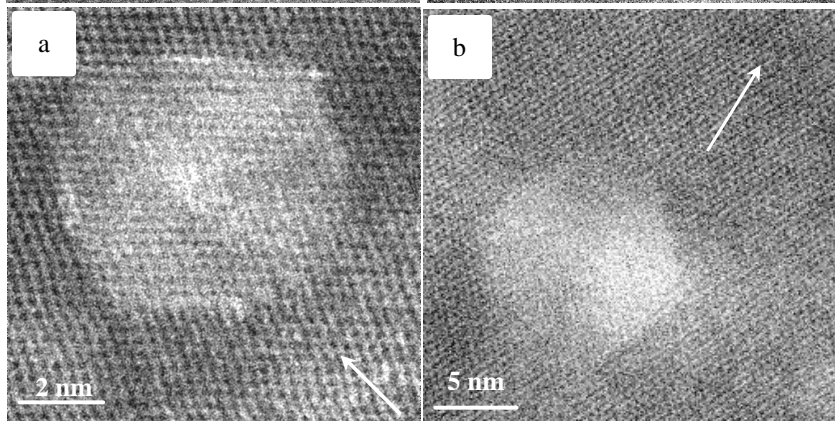


Figure 5: [110] cross section Z-contrast STEM images, $x = 0.1$, ex-situ annealed; (a) void in Si, lined on its interface with the Si matrix by Sn; (b) partially formed $\text{Sn}_x\text{Si}_{1-x}$ precipitate in Si with $x > 0.1$, grown by phase separation from a $\text{Sn}_{0.1}\text{Si}_{0.9}$ layer. The arrows represent the respective growth directions.

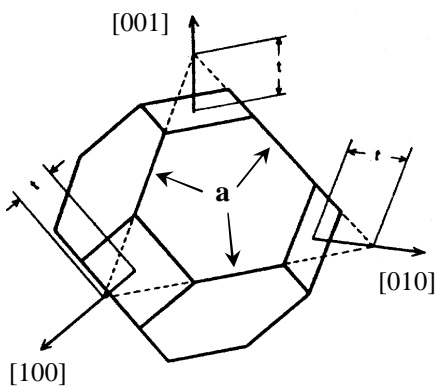


Figure 6: Sketch of a tetrakaidecahedron after ref. 16. This shape is determined by $\{111\}$, i.e. octahedron, and $\{100\}$, i.e. cube, planes. $A = 1/a$ is a shape parameter; for $A = 0$ the shape is an octahedron and $A = 2/3$ corresponds to a cube. Calculating the point group of the interface energy density by means of Neumann's symmetry principle results in the possible precipitates' shapes: tetrakaidecahedron, octahedron, cube, and sphere. While the shapes of small precipitates are likely to be determined by the anisotropy of the interface energy, the shapes of larger precipitates are likely to be determined by the anisotropy of the lattice mismatch strain energy [16].

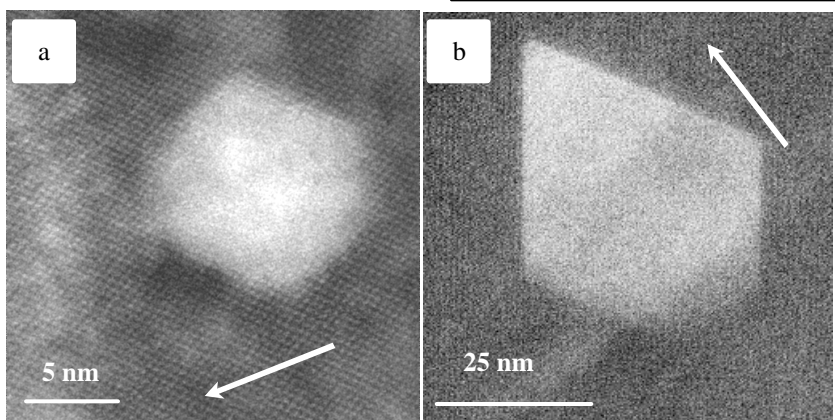


Figure 7: Shape transition of Sn QDs in Si (a) tetrakaidecahedron as dominated by the anisotropy of the interface energy density; (b) essentially octahedron as dominated by the anisotropy of the elastic mismatch strain energy. The arrows represent the respective growth directions.

An interesting question is how these voids may have arisen in the first place. The possible answer to this question may be found in a mechanism analogously to that described in ref. 18, which states that when a freshly prepared Si surface is exposed to air, voids of about 10 nm diameter and a number density of about 10^{10} cm^{-2} form spontaneously approximately 10 nm below the surface due to compressive strain that arises from the formation of SiO_2 on the surface. Deposited $\text{Sn}_x\text{Si}_{1-x}$ layers may also cause the formation of voids during the growth process since they also compress a freshly grown Si surface. Finally, the thermal cycling during temperature and growth rate modulated MBE [8,9] of multilayer structures ensures that there is no shortage of vacancies in the structure and this could allow preformed voids of any shape to grow and reach their equilibrium shape.

Phase separation of Sn from a pseudomorph $\text{Sn}_x\text{Si}_{1-x}$ predecessor layer, result in QDs as well since the diamond structural prototype can be conserved. Fig. 5b shows an early stage of the formation of such a QD at the spatial position of a pseudomorph $\text{Sn}_{0.1}\text{Si}_{0.9}$ layer. The chemical composition and compositions range of such QDs are, however, unclear. When fully formed, these QDs may be substitutional solid solutions of Sn in Si with a much higher Sn content than the pseudomorph $\text{Sn}_x\text{Si}_{1-x}$ predecessor layers. This mechanism is considered the second formation mechanism for QDs in the Sn/Si system. Note that only for a very high Sn content, larger than 90 %, is a direct band gap predicted for $\text{Sn}_x\text{Si}_{1-x}$ alloys [3].

A shape transition with size of Sn rich precipitates that is probably due to an increasing contribution of the elastic mismatch strain energy to the total energy of the QDs has been observed, Fig. 7. While smaller Sn rich precipitates possess the typical tetrakaidecahedron shape, Figs. 5b, 6, and 7a (which probably results from the anisotropy of the interface energy density), a much larger Sn (rich) precipitate had a shape that resembles more closely an octahedron, Fig. 7b. The shape of this large precipitate probably results from the anisotropy of the elastic mismatch strain energy. Intermediately sized Sn rich precipitates possessed tetrakaidecahedron shapes with smaller {001} facets, i.e. smaller shape parameters A, see caption of Fig. 6, indicating a gradual transition to the shape of an octahedron ($A = 0$) with increasing size. As this large precipitate was partly observed at the predecessor substitutional $\text{Sn}_{0.1}\text{Si}_{0.9}$ solution layer and partly within the Si spacer layer, it may have formed by the simultaneous operation of both mechanisms. The upper part of the QD may, therefore, consist of a-Sn and the lower part of a substitutional solution with a high Sn content. This hypothesis is consistent with the Z-contrast image seen in Fig. 7b. Finally, we would like to suggest that the employment of the void creation and subsequent filling mechanism (by with a-Sn QDs form in Si) may offer an opportunity to make progress in other (less severely strained) QD systems such as InAs QDs in Si.

4. Conclusions

Two mechanisms for the formation of quantum dots in the Sn/Si system have been proposed. The first of these mechanisms involves the creation of voids in the Si matrix and their subsequent filling with Sn atoms by diffusion. The second mechanisms results from phase separation. While the QDs that result from the first mechanism consist of pure a-Sn, the quantum dots that result from the second mechanism are probably substitutional $\text{Sn}_x\text{Si}_{1-x}$ alloys with a high Sn content. Both of these mechanisms result in QDs which possess the diamond structure and the typical shape of a tetrakaidecahedron. As the chemical compositions and composition distributions of the QDs are not known at present, further experiments are to be undertaken in order to clarify this issue.

Acknowledgments

Alan Nicholls (Electron Microscopy Service, University of Illinois at Chicago, UIC) is thanked for experimental support. This research was supported by both a grant to NDB by the National Science Foundation (DMR-9733895) and a grant to PM by the Campus Research Board of UIC.

References

- [1] D. Bimberg, "Quantum dots: Paradigm changes in semiconductor physics", *Semiconductors* **33**, 951-955 (1999).
- [2] N.N. Ledentsov, V.M. Ustinov, V.A. Shchukin, P.S. Kop'ev, Zh.I. Alferov, and D. Bimberg,

- “Quantum dot heterostructures: fabrication, properties, lasers (Review)”, *Semiconductors* **32**, 343-365 (1998).
- [3] R.A. Soref and C.H. Perry, “Predicted band gap of the new semiconductor SiGeSn”, *J. Appl. Phys.* **69**, 539-541 (1991).
- [4] S.Y. Shiryayev, J. Lundsgaard Hansen, P. Kringhøj, and A.N. Larsen, “Pseudomorphic Si_{1-x}Sn_x alloy films grown by molecular beam epitaxy on Si”, *Appl. Phys. Lett.* **67**, 2287-2289 (1995).
- [5] M.F. Flynn, J. Chevallier, J. Lundsgaard Hansen, and A. Nylandsted Larsen, “Relaxation of strained, epitaxial Si_{1-x}Sn_x”, *J. Vac. Sci. Technol. B* **16**, 1777-1785 (1998).
- [6] M.F. Flynn, J. Chevallier, A. Nylandsted Larsen, R. Feidenhans'l, and M. Seibt, “ α -Sn and β -Sn precipitated in annealed Si_{0.95}Sn_{0.05}”, *Phys. Rev. B* **60**, 5770-5777 (1999).
- [7] C. Ridder, M. Fanciulli, A. Nylandsted Larsen, and G. Weyer, “Precipitation of Sn in metastable, pseudomorphic Si_{0.95}Sn_{0.05} films grown by molecular beam epitaxy”, *Mater. Sci. Semicond. Processing* **3**, 251-255 (2000).
- [8] K.S. Min and H.A. Atwater, “Ultrathin pseudomorphic Sn/Si and Sn_xSi_{1-x}/Si heterostructures”, *Appl. Phys. Lett.* **72**, 1884-1886 (1998).
- [9] R. Ragan, K.S. Min, and H.A. Atwater, “Direct energy gap group IV semiconductor alloys and quantum dot arrays in Sn_xGe_{1-x}/Ge and Sn_xSi_{1-x}/Si alloy systems”, *Mater. Sci. Engin. B* **87**, 204-213 (2001).
- [10] For hydrostatic pressure, the product of the bulk modulus (42.6 GPa for α -Sn and 70.2 GPa for Sn_{0.5}Si_{0.5} assuming Vegard's law applicable) and the relative elastic volume change is equal to the product of pressure and volume, which is also the excess Gibbs free energy due to lattice mismatch strains. Starting with an unstrained α -Sn sphere of 10 nm diameter (with lattice constant 0.6489 nm) that contains 15329 atoms, one obtains for a relative elastic volume change of 19.5 % a pressure of 8.3 GPa and an excess Gibbs free energy of 1.77 eV per atom. For a same diameter Sn_{0.5}Si_{0.5} sphere (with lattice constant 0.596 nm, assuming Vegard's law applicable) that contains 19785 atoms, one obtains for a 9.75 % relative elastic volume change a pressure of 6.84 GPa and an excess Gibbs free energy of 1.13 eV per atom. The usage of this simple formula is justified by studies of the size dependency of elastic properties of nanometer sized particles, e.g. S.P. Baker, R.P. Vinci, and T. Arias, “Elastic and Anelastic Behavior of Materials in Small Dimensions”, *MRS Bulletin* **27**, No. 1, 26-29 (2002) and R.E. Miller and V.B. Shenoy, “Size-dependent elastic properties of nanosized structural elements”, *Nanotechnology* **11**, 139-147 (2000).
- [11] This hydrostatic pressure range is known to lead to structural transformations in elemental (group IV) and binary III-V compound semiconductors; see, e.g., G.J. Ackland, “High-pressure phases of group IV and III-V semiconductors”, *Rep. Prog. Phys.* **64**, 483-516 (2001).
- [12] P. Möck, Y. Lei, T. Topuria, N.D. Browning, R. Ragan, K.S. Min, and H.A. Atwater, “Structural Transformations in self-assembled Semiconductor Quantum Dots as inferred by Transmission Electron Microscopy”, *Proc. of 47th Annual Meeting of The International Society for Optical Engineering (SPIE), Symposium “Physical Chemistry of Interfaces and Nanomaterials”*, 7-11 July, 2002, Seattle, WA.
- [13] D.A. Porter and K.E. Easterling, *Phase Transformations in Metals and Alloys*, Chapman & Hall, London, New York, 1992.
- [14] Y. Lei, P. Möck, T. Topuria, N.D. Browning, R. Ragan, K.S. Min, and H.A. Atwater, *in preparation*.
- [15] D.J. Eaglesham, A.E. White, L.C. Feldman, N. Moriya, and D.C. Jacobson, “Equilibrium Shape of Si”, *Phys. Rev. Lett.* **70**, 1643-1646 (1993).
- [16] W.C. Johnson, “Influence of Elastic Stress on Phase Transformations”, in: *Lectures on the Theory of Phase Transformations*, 2nd Edition, Ed. H.I. Aaronson, The Minerals, Metals & Materials Society, Warrendale, 2001.
- [17] As the pressure on the precipitates is in a first approximation hydrostatic, i.e. isotropic, Curie's symmetry principle, e.g. ref. 16, yields no influence of the misfit stress field on the anisotropy of the interface energy density.
- [18] S. Lin, I. Mack, N. Pongkrapan, and P. Fraundorf, “Ten-nanometer surface intrusions in room temperature silicon”, *Electrochem. Solid-State Sci. Lett.* in press (2002), con-mat/0110393.